Research Article | Vol. 24, No. 26 | 26 Dec 2016 | OPTICS EXPRESS 29948

Optics EXPRESS

Enhanced fourth harmonic generation via nonlinear Čerenkov interaction in periodically poled lithium niobate crystal

XIN CHEN,[1] KRZYSZTOF SWITKOWSKI,[2,3] XIAOPENG HU,[4] WIESLAW KROLIKOWSKI,[1,3] AND YAN SHENG[1*]

[1]*Laser Physics Center, Research School of Physics and Engineering, Australian National University, Canberra ACT 2601, Australia*
[2]*Faculty of Physics, Warsaw University of Technology, Warsaw, Poland*
[3]*Science Program, Texas A&M University at Qatar, Doha, Qatar*
[4]*National Laboratory of Solid State Microstructures, Nanjing University, Nanjing 210093, China*
[*]*yan.sheng@anu.edu.au*

Abstract: We introduce a custom-cut periodically poled ferroelectric crystal for the phase matching of multistep cascading frequency conversion processes. Our approach involves combination of collinear second harmonic generation and transverse sum frequency mixing via the total internal reflection of the fundamental and collinear second harmonic beams. As a proof of concept we demonstrate multiple frequency generation with an enhanced fourth harmonic signal in a one-dimensional periodically poled $LiNbO_3$ crystal.

OCIS codes: (190.2620) Harmonic generation and mixing; (190.4160) Multiharmonic generation.

References and links

1. J. A. Armstrong, N. Bloembergen, J. Ducuing, and P. S. Pershan, "Interactions between light waves in a nonlinear dielectric," Phys. Rev. Lett. **127**(6), 1918–1939 (1962).
2. M. M. Fejer, G. A. Magel, D. H. Jundt, R. L. Byer, "Quasi-phase-matched second harmonic generation: tuning and tolerances," IEEE J. Quantum Electron. **28**(11) 2631–2654 (1992).
3. I. Freund, "Nonlinear diffraction," Phys. Rev. Lett. **21**(19), 1404–1406 (1968).
4. S. Saltiel, Y. Sheng, N. Voloch-Bloch, D. Neshev, W. Krolikowski, A. Arie, K. Koynov, and Y. Kivshar, "Cerenkov-type second-harmonic generation in two-dimensional nonlinear photonic structures," IEEE J. Quantum Electron. **45**, 1465–1472 (2009).
5. K. Kalinowski, P. Roedig, Y. Sheng, M. Ayoub, J. Imbrock, C. Denz, and W. Krolikowski, "Enhanced Čerenkov second-harmonic emission in nonlinear photonic structures," Opt. Lett. **37**(11), 1832–1835 (2012).
6. P. Molina, M. O. Ramirez, B. J. Garcia, and L. E. Bausa, "Directional dependence of the second harmonic response in two-dimensional nonlinear photonic crystals," Appl. Phys. Lett. **96**, 261111 (2010).
7. Y. Sheng, Q. Kong, V. Roppo, K. Kalinowski, Q. Wang, C. Cojocaru, J. Trull, and W. Krolikowski, "Theoretical study of Čerenkov-type second-harmonic generation in in periodically poled ferroelectric crystals," J. Opt. Soc. Am. B **29**, 312–318 (2012).
8. N. An, Y. Zheng, H. Ren, X. Deng, and X. Chen, "Conical second harmonic generation in one-dimension nonlinear photonic crystal," Appl. Phys. Lett. **102**(20), 201112 (2013).
9. M. Ayoub, P. Roedig, J. Imbrock, and C. Denz, "Domain-shape-based modulation of Čerenkov second-harmonic generation in multidomain strontium barium niobate," Opt. Lett. **36**, 4371–4373 (2011).
10. Y. Sheng, V. Roppo, K. Kalinowski, and W. Krolikowski, "Role of localised modulation of $\chi^{(2)}$ in Čerenkov second harmonic generation in nonlinear bulk medium," Opt. Lett. **37**, 3864–3866 (2012).
11. K. Kalinowski, Q. Kong, V. Roppo, A. Arie, Y. Sheng, W. Krolikowski, "Wavelength and position tuning of Čerenkov second harmonic generation in optical superlattice," Appl. Phys. Lett. **99**(18), 181128 (2011).
12. V. Roppo, K. Kalinowski, Y. Sheng, W. Krolikowski, C. Cojocaru, and J. Trull, "Unified approach to Čerenkov second harmonic generation," Opt. Express **21**(22), 25715–25726 (2010).
13. X. Deng and X. Chen, "Domain wall characterization in ferroelectrics by using localized nonlinearities," Opt. Express **18**, 15597–15602 (2010).
14. Y. Sheng, A. Best, H. Butt, W. Krolikowski, A. Arie, and K. Koynov,"Three-dimensional ferroelectric domain visualization by Čerenkov-type second harmonic generation," Opt. Express **18**, 16539–16545 (2010).
15. P. Karpinski, X. Chen, V. Shvedov, C. Hnatovsky, A. Grisard, E. Lallier, B. Luther-Davies, W. Krolikowski, Y. Sheng, "Nonlinear diffraction in orientation-patterned semiconductors," Opt. Express **23**, 14903–14912 (2015).

#277996 http://dx.doi.org/10.1364/OE.24.029948
Journal © 2016 Received 3 Oct 2016; revised 7 Dec 2016; accepted 8 Dec 2016; published 16 Dec 2016

Optics EXPRESS

16. Y. Sheng, W. Wang, R. Shiloh, V. Roppo, Y. Kong, A. Arie, and W. Krolikowski, " Čerenkov third-harmonic generation in $\chi^{(2)}$ nonlinear photonic crystal," Appl. Phys. Lett. **98**(24), 241114 (2011).
17. C. D. Chen, J. Lu, Y. H. Liu, X. P. Hu, L. N. Zhao, Y. Zhang, G. Zhao, Y. Yuan, and S. N. Zhu, " Čerenkov third-harmonic generation via cascaded $\chi^{(2)}$ processes in a periodic-poled $LiTaO_3$ waveguide," Opt. Lett. **36**(7), 1227–1229 (2011).
18. M. Ayoub, P. Roedig, J. Imbrock, and C. Denz, "Cascaded Čerenkov third-harmonic generation in random quadratic media," Appl. Phys. Lett. **99**(24), 241109 (2011).
19. L. Mateos, P. Molina, J. Galisteo, C. Lopez, L. E. Bausa, M. O. Ramirez, "Simultaneous generation of second to fifth harmonic conical beam in a two-dimensional nonlinear photonic crystal," Opt. Express **20**(28), 29940–29948 (2012).
20. N. An, H. Ren, Y. Zheng, X. Deng, X. Cheng, "Čerenkov high-order harmonic generation by multistep cascading in $\chi^{(2)}$ nonlinear photonic crystal," Appl. Phys. Lett. **100**(22), 221103 (2012).
21. D.E. Zelmon, D.L. Small, and D. Jundt, "Infrared corrected Sellmeier coefficients for congruently grown lithium niobate and 5% magnesium oxide-doped lithium niobate," J. Opt. Soc. Am. B **14**(12), 3219–3222 (1997).
22. A. M. Weiner, "Effect of group velocity mismatch on the measurement of ultrashort optical pulses via second harmonic generation," IEEE J. Quantum Electron. **19**(8), 1276–1283 (1983).
23. Y. Sheng, J. Dou, B. Ma, and D. Zhang, "Broadband efficient second harmonic generation in media with a short-range order," Appl. Phys. Lett. **91**(1), 011101 (2007).

1. Introduction

The quasi-phase matching (QPM) technique [1, 2] in periodically poled ferroelectric crystals or orientation-patterned semiconductors has been widely used in optical frequency conversion, wave-front manipulation, and ultrafast signal processing. It is based on spatial modulation of the second-order nonlinear coefficient $\chi^{(2)}$ of the material to create a set of reciprocal lattice vectors to compensate for the phase mismatch in a nonlinear wave mixing process. The simplest process of collinear second harmonic generation (SHG) is illustrated in Fig. 1(a). Here the quasi-phase matching condition can be written as $k_2 - 2k_1 - G_m = 0$, where k_1 and k_2 are wave vectors of fundamental and second harmonic waves, respectively, and $G_m = 2m\pi/\Lambda$ (m = 0,1,2...) with Λ being period of the $\chi^{(2)}$ modulation.

Apart from the typical collinear interaction, QPM has been also widely employed in non-collinear (or transverse) interaction geometry. In this case, the fundamental beam propagates normally to the $\chi^{(2)}$ modulation, while the generated harmonic waves are emitted in the transverse direction. In the example illustrated in Fig. 1(b), for a fundamental beam propagating exactly normally to periodic $\chi^{(2)}$ modulation the nonlinear interaction leads to a number of second harmonics with wavevectors k_{2m} emitted at angles such that $k_{2m}\sin\alpha_m - G_m = 0$. This process resembles traditional Raman-Nath diffraction of light on index grating and hence is termed nonlinear Raman-Nath diffraction [3]. The efficiency of this process is rather low because for each emitted beam only the transverse phase matching condition is fulfilled, while the nonzero phase mismatch along the propagation direction leads to periodic energy flow between fundamental and second harmonics. However, as the experiments show, in addition to low intensity Raman-Nath SH peaks there are also a pair of strong beams, the so-called Čerenkov, emitted with the wave vector k_{2C} such that $k_{2C}\cos\theta_C - 2k_1 = 0$ [4, 5], where θ_C is the angle at which Čerenkov beam is emitted. Unlike the nonlinear Raman-Nath emission whose direction is governed by the spatial periodicity of $\chi^{(2)}$ through reciprocal lattice vectors G_m , the direction of the Čerenkov beam is determined solely by the fulfilment of the longitudinal phase matching condition. Since, by definition, the longitudinal phase matching is satisfied for Čerenkov beam, this beam experiences monotonic growth in propagation and hence its intensity can be quite high. The Čerenkov SHG has been already discussed and observed in various nonlinear media [6–9]. While Čerenkov emission may, in principle, take place in a homogeneous nonlinear medium, any sharp (even, isolated) nonlinearity modulation, such as periodic or chirped $\chi^{(2)}$ gratings greatly facilitate the process [10–13]. This made it attractive for applications in second harmonic microscopy, where it provides remarkable enhancement of contrast allowing for three-dimensional diagnostics of $\chi^{(2)}$ nonlinearity patterns in nonlinear

Optics EXPRESS

crystals [14, 15].

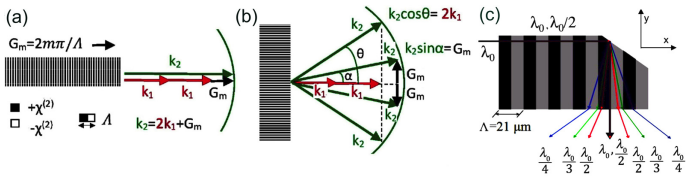

Fig. 1. (a,b) Phase matching diagrams of (a) traditional collinear quasi-phase matched SHG and (b) transverse SHG. The arc represents the magnitude of the SH wave vector; α is the emission angle of m-th Raman-Nath SH wave, and θ is the Čerenkov SH emission angle that is determined solely by the longitudinal phase matching condition. (c) The geometry of multiple frequency mixing process that combines both, collinear and transverse types of interactions. Here the collinear SH generation is followed, after its total reflection at the 45° corner, by the Čerenkov second-, third-, and fourth-harmonic generations.

Because of its relatively high efficiency, Čerenkov interaction is attractive for frequency conversion. In particular, one can utilize sum frequency mixing involving fundamental and Čerenkov beams to generate higher harmonics of the single fundamental beam [16–18]. Starting with long wavelength fundamental beam such cascading process of sum frequency mixing has generated up to fifth harmonic of the original input wavelength [19, 20]. Moreover, because of material dispersion each generated harmonic is emitted at different angle leading to the formation of the so-called nonlinear colour fan. The major drawback of this, and other transverse interaction schemes is the quick decrease of conversion efficiency with increased cascading order. Therefore the power of higher harmonics becomes progressively the weaker. In contrast, phase matched collinear frequency generation in periodically poled structures ensures strong energy transfer between the fundamental and its second harmonic.

In this work, we propose to combine traditional collinear QPM interaction with nonlinear Čerenkov frequency generation in a single sample of periodically poled nonlinear crystal. Our approach offers the advantages of both interaction mechanisms to achieve higher efficiency of high harmonic generation via $\chi^{(2)}$ cascading. As a proof of concept we demonstrate enhanced fourth harmonic generation in a custom-cut periodically poled lithium niobate crystal.

2. Theoretical design

The geometry of the proposed nonlinear optical interaction is schematically depicted in Fig. 1(c). The rectangular shaped z-cut sample of ferroelectric crystal (Lithium niobate, $LiNbO_3$) has one of its corners cut at 45°. The sample is periodically poled with period Λ along the, say, x axis. The fundamental beam (wavelength λ_0) propagates along the same axis until it is totally internally reflected at the 45° cut corner. After that the beam propagates along y-direction and finally leaves the sample. The nonlinear interaction in the crystal can be divided into two stages. Firstly, the input fundamental beam (FB) efficiently generates its second harmonic (SH) via quasi-phase matched collinear interaction using G_1 [Fig. 1(a)]. To this end the poling period satisfies the following condition: $\Lambda = \lambda_0/2(n_{e,2} - n_{e,1})$, where $n_{e,1}$, $n_{e,2}$ are extraordinary refractive indices of $LiNbO_3$ at the wavelengths of FB and SH, respectively. At the end of this collinear interaction both, FB and strong SH experience the total internal reflection, after which they propagate normally to the periodic $\chi^{(2)}$ modulation. During this second stage of propagation both beams serve as sources of transversely emitted higher harmonics as shown in Fig. 1(c). Due to periodicity of the $\chi^{(2)}$ structure the transverse interaction involves both Raman-Nath and Čerenkov harmonic emissions. The effect of nonlinear Raman-Nath emission in sum frequency mixing has been discussed in detail in [19]. Since it is much weaker than the Čerenkov, we will neglect it in further discussions. Therefore, we are left with seven

Optics EXPRESS

Čerenkov frequency conversion processes, schematically depicted in Figs. 2(b-h) in terms of phase matching conditions. Here we do not consider Čerenkov SHG at the boundary between crystal and air in total internal reflection [12], which is expected to be much weaker than that caused by periodic $\chi^{(2)}$ modulation.

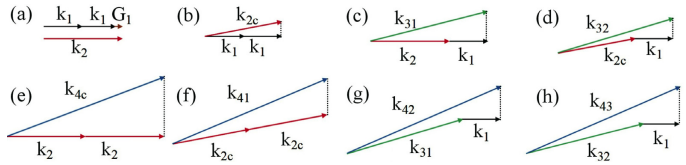

Fig. 2. Phase matching diagrams of frequency conversions in the customized structure. (a) Quasi-phase matched collinear SHG; (b) Čerenkov SHG; (c,d) Čerenkov THG via sum frequency mixing involving collinear and Čerenkov SH, respectively; (e,f) Čerenkov FHG via frequency doubling of collinear and Čerenkov SH, respectively; and (g,h) Čerenkov FHG via sum frequency mixing of the fundamental and different third harmonics.

Firstly, frequency doubling of collinear FB and SH results in appearance of Čerenkov second [Fig. 2(b)] and Čerenkov fourth [Fig. 2(e)] harmonics, with wave vectors $\mathbf{k}_{2c}$ and $\mathbf{k}_{4c}$, respectively. The subsequent sum frequency mixing between FB and both, collinear SH and transverse Čerenkov SH leads to generations of two third harmonic waves with wave vectors $\mathbf{k}_{31}$ and $\mathbf{k}_{32}$, respectively [see Figs. 2(c) and 2(d)]. There are three additional contributions to the forth harmonic generation. They include the wave formed via direct frequency doubling of Čerenkov second harmonic ($\mathbf{k}_{41}$) [Fig. 2(f)], and the other two formed via sum frequency mixing of the two third harmonics and the fundamental beam, denoted as $\mathbf{k}_{42}$ and $\mathbf{k}_{43}$ [Figs. 2(g) and 2(h)], respectively. Following the analysis above one can determine the emission angle for each harmonic. These angles along with the corresponding formulas, for which the Sellmeier equation of $LiNbO_3$ [21] was used, are listed in Table 1. It is clearly seen that the emission angles of the Čerenkov harmonic waves depend only on the refractive indices of the material.

Table 1. Internal emission angles of the Čerenkov harmonics

Angles	θ_{2C}	θ_{31}	θ_{32}	θ_{4C}	θ_{41}	θ_{42}	θ_{43}
Theory	10.84°	14.31°	16.76°	20.78°	23.33°	23.33°	22.09°
Measurement	11.38°	14.96°	16.75°	21.26°			
$\cos\theta =$	$\frac{n_{e,1}}{n_{e,2}}$	$\frac{n_{e,1}+2n_{e,2}}{3n_{e,3}}$	$\frac{n_{e,1}}{n_{e,3}}$	$\frac{n_{e,2}}{n_{e,4}}$	$\frac{n_{e,1}}{n_{e,4}}$	$\frac{n_{e,1}}{n_{e,4}}$	$\frac{n_{e,1}+n_{e,2}}{2n_{e,4}}$

3. Experiment and results

In the experiment we used a z-cut periodically poled lithium niobate crystal fabricated via electric-field poling technique. The sample's dimensions are 23 mm (x)×7 mm(y)× 0.5 mm(z), respectively. The poling period was Λ = 21 μm with duty factor of 50% for the most efficient collinear second harmonic generation at fundamental wavelength of λ_0 = 1620 nm. One of the sample's corners was cut at 45° and the resulting plane was polished to ensure total internal reflection of both fundamental and SH beams. The 150 fs beam (25 nm bandwidth) from optical parametric amplifier (Coherent OPerA Solo, 1 kHz rep. rate) was first expanded and then loosely focused with the plano-convex lens (f = 500 mm) at the X facet of the crystal. The focal spot (roughly 100 μm wide) was located in the middle of the sample. With this width at least 5 periods of $\chi^{(2)}$ modulations were covered by the beam. The extraordinary input polarization ensured the strongest (ee-e) nonlinear interaction. The beam propagated through the sample

Optics EXPRESS

for 20 mm along the *x*-direction until it was totally internally reflected at 45° surface and propagated along the *y*-direction (parallel to ferroelectric domain walls) for the next 5 mm, and finally left the sample. The emitted beams were projected onto the screen which was imaged with a CCD camera. The Glan prisms and half wave-plate were used to control the input beam power. To avoid material damage the average input power was kept at a level of 150 μW.

On illuminating the sample with fundamental beam we clearly observed a number of harmonic beams emitted from the *Y*-surface of the sample as shown in Fig. 3(a). All beams were extraordinary polarized owing to the (ee-e) nonlinear interaction. The central spot represents both, fundamental and collinearly generated quasi-phase matched second harmonic. As the conversion efficiency of the collinear interaction reached 36%, both beams were of quite high intensity and had to be attenuated in order to make other beams visible on the CCD. The average power of the collinear SH was 55 μW. The bright, transversely emitted beams that are closest to the central spots are Čerenkov second harmonics (CSH) with an average power of 0.9 μW. Next, there is a pair of green spots representing third harmonic beams (TH_1, TH_2) whose phase matching processes are depicted in Figs. 2(c) and 2(d), respectively. Their combined power was 7.78 nW. These TH beams are significantly weaker than CSH. In fact, we could expect the beam TH_2 to be much weaker because it originates from the second cascading order of interaction. The beam TH_1 formed via sum frequency mixing of two strong beams, fundamental and collinear SH, and hence was expected to be relatively strong. Its low power is most likely caused by the use of short pulses (150 fs) in our experiments. In this regime the frequency conversion process is adversely affected by the group velocity mismatch between the fundamental and second harmonic pulses, which is estimated to be 0.27 ps/mm at 1620 nm for congruent $LiNbO_3$ crystal. The mismatch restricted the effective interaction distance. One may expect to achieve higher conversion efficiency for TH_1 by using longer (picosecond or nanosecond) pulses [22].

Finally there is a pair of strong blue spots representing fourth harmonics of the fundamental wave. Its combined power was 57 nW. In the traditional scheme of cascading of nonlinear processes the fourth harmonic should be much weaker than the third harmonics. This is not the case here since the major contribution to the FH comes from Čerenkov frequency doubling of the collinearly emitted SH. The order of this process is the same as Čerenkov SHG and hence the beam intensity is few times higher than the intensity of the third harmonic. Notice that the group velocity mismatch does not affect the Čerenkov fourth harmonic, as only the collinear second harmonic serves as the major source of the emission [see Fig. 2 (e)].

The measured internal emission angles for these harmonic beams, listed in Table 1, agree well with the theoretical values. Interestingly, we observed only one broad spot corresponding to the fourth harmonic generation. Therefore, the angle 21.26° refers to the maximum in the blue emission spot. Because of its 2.72° angular width, it most likely corresponds mainly to $\mathbf{k}_{4C}$ and $\mathbf{k}_{43}$ emission. The two other beams with wave-vectors $\mathbf{k}_{41}$ and $\mathbf{k}_{42}$ should be emitted at an angle close to the angle of total internal reflection. Therefore these beams could be either trapped inside the sample or significantly attenuated due to the Fresnel reflection at the boundary. We attribute the small difference between measured and predicted emission angles to departure of the direction of fundamental beam from the ideal normal incidence inside the sample. While Čerenkov harmonic emission is always symmetric with respect to ferroelectric domain walls, any tilt of the fundamental beam (in the plane of the structure) leads to increased emission angle and angularly asymmetric emission with respect to the direction of fundamental beam [5]. From our measurements we estimated the angular tilt of the fundamental beam to be approximately 4°. The asymmetry of Čerenkov emission with respect to propagation direction of the fundamental beam, is clearly visible in Fig. 3(a). Moreover, in agreement with theory [5] the tilt of fundamental beam also causes asymmetric power distribution within the pair of Čerenkov beams, which is also evident in Fig. 3(a), where all beams propagating to the right

Optics EXPRESS

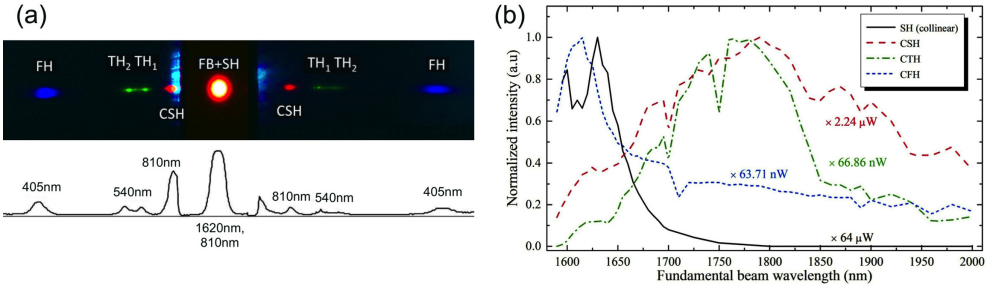

Fig. 3. (a) Experimentally recorded angular distribution of multiple frequency signals. The central spot corresponds to overlapping fundamental and collinearly generated SH beams. The latter is shown using false red color. Due to large differences in the harmonic powers this is a composite picture with enhanced brightness and contrast of high harmonics. The vertical bright streaks around CSH beams are artefacts caused by scattering of the fundamental beam in the sample. (b) Normalized intensity of the constituent harmonics as a function of the wavelength of fundamental beam. Numerical factors next to the plots represent the maximal power of each beam.

of FB are stronger than their left counterparts. In fact, this property can be utilised in directing majority of emitted power into one set of Čerenkov beams.

In Fig. 3(b) we depict measured intensity of each emitted harmonics as a function of the wavelength of the fundamental beam. All curves are normalized to their maxima. It is clear that departure from the exact resonant wavelength (1620 nm) results in an immediate drop of the collinear SH and Čerenkov FH, indicating again that the collinear SH serves as the major emission source of the fourth harmonic generation [Figs. 2(e)]. Note that the FH did not vanish even though the collinear SH became weak at longer wavelengths. This indicates the growing contributions to FH from the other phase matching processes, namely those involving the Čerenkov SHG [Figs. 2(f-h)], which became stronger at longer wavelengths. The plot in Fig. 3(b) also shows the nonmonotonic dependence of Čerenkov TH and SH on the fundamental wavelength. This agrees with the fact that the Čerenkov frequency generation in a periodic structure strongly depends on the wavelength [10]. For certain wavelengths, both transverse and longitudinal phase matching conditions will be simultaneously satisfied, giving rise to the nonlinear Bragg diffraction which will enhance the Cerenkov emission [5]. In fact, the growth of CSH and CTH for longer wavelengths, seen in Fig. 3(b) is very likely caused by this effect as we determined that Bragg resonances appear at 1680 nm and 1800 nm. The wavelength sensitivity could be weakened by incorporating weak disorder into the otherwise periodic domain pattern [11]. Moreover, the disorder could significantly broaden the bandwidth of our technique by easing the inherently narrow spectral response of collinear interaction [23]. Finally, the central frequency of our custom-cut ferroelectric crystal can be tuned by angular tilting of the incident fundamental beam. The tilting would also enhance the Čerenkov emission at angles corresponding to the Bragg nonlinear diffraction [5].

4. Conclusion

We studied multiple frequency generation via the nonlinear cascading process in nonlinear photonic structure. By employing the total internal reflection inside the sample we combined quasi-phase matched collinear and Čerenkov nonlinear sum frequency mixing to realize enhanced fourth harmonic generation in a single periodically poled lithium niobate crystal.

Optics EXPRESS

Funding

China Scholarship Council (X.Chen's PhD Scholarship No. 201306750005); Australian Research Council; Qatar National Research Fund (Grant No. NPRP 8-246-1-060); National Natural Science Foundation of China (Grant No. 11674171).